MARA 10: An integral model experiment in support of LMFBR containment analyses

J.Louvet & P.Hamon
Commissariat à l'Energie Atomique, CEN Cadarache, DRNR, St-Paul-lez-Durance, France
B.L.Smith
Swiss Federal Institute for Reactor Research, Würenlingen
A.Zucchini
ENEA, CSR E.Clementel, Bologna, Italy

1 INTRODUCTION

In the framework of HCDA safety analysis for the SUPERPHENIX reactor LMFBR, containment code validation has been carried out at CEA by means of the MARA experimental program, consisting of ten 1/30 scale model tests.

Early tests in the series comprised simple bare tank configurations, but then progressively more complex tests were performed with internal components and deforming roof added step by step.

The last test in the series, MARA 10, is an integral model experiment which involves different kinds of deformable structures :

- vessel, as in MARA 01/02, /1/ ;
- core support and diagrid, as in MARA 04, /2/ ;
- deforming roof, as in MARA 08, /3/ ;
- above core structure (ACS) ;
- radial shield.

The aim of the paper is to present the experimental results of the MARA 10 test, compare these to different code calculations, and to point out the most important effects of structures surrounding the bubble on the general response of primary containments to HCDA loadings.

2 EXPERIMENTAL SET-UP

All tests of the MARA series have been fired in identical 316 steel vessels of 1.2 mm thickness using a 45 g low density, low pressure explosive charge, /4/.

In MARA 10 (figure 1), the flexible roof of 10 mm thickness A42 steel is clamped to the roof support as in MARA 08. The vessel is welded to a flange which is bolted to the roof support.

The core support structure is machined from a single block of Au 4g aluminium. It is supported by a thin collar attached to the vessel base.

The diagrid is a 304L steel plate of 8.8 mm thickness just resting under gravity on the inner flange of the core support.

The radial shield is represented by a deformable A316 steel cylindrical vessel of 200 mm diameter. The vessel base is welded to a flange which is clamped by bolts to the diagrid. The vessel thickness decreases from the base (6.5 mm) to the top (2 mm) in order to allow the structure to deform conically. In addition, the vessel thickness is locally reduced at its base to try to simulate a pinned attachment with the diagrid.

The above core structure (ACS) is a 1 mm thick deformable A316 cylinder of 140 mm diameter and 210 mm height, completly filled with water to avoid buckling of the wall as a

consequence of the base (also 1 mm thick) deflection. The ACS is securely clamped to the deformable roof by bolts. The welded corner between wall and base plate is stiffened to avoid rupture. The explosive charge is supported at the base of the structure.

The main vessel is partially filled with water leaving an air gap of 35 mm at the top.

The whole test is well instrumented with :

- 7 pressure transducers fitted under the roof at different radii,
- 8 strain gauges placed on the upper and lower sides of the roof at three radial locations (center, mid-radius and near the boundary) to measure axial and hoop strains,
- 5 strain gauges attached at the three main locations on the vessel (upper bulge, charge level and base) to obtain axial and hoop strains,
- 6 strain gauges placed on internal structures :
  2 on the above core structure (bottom and wall),
  2 on the radial shield (charge level and top),
  1 under the diagrid center,
  1 on the collar supporting the matting,
- 2 high speed cameras used to obtain displacements of the roof and the vessel (upper bulge and base),
- residual deformations are evaluated by measuring, before and after firing, mesh sizes of grids drawn on the different structures.

3 EXPERIMENTAL RESULTS

After dismantling the internal structures we can observe that :

- The radial shield has its maximum radial deformation at charge height. The expected flowering effect is not obtained though the hinge, simulated at the shield base by a thickness reduction, has worked correctly. In addition, the entire cylindrical surface of the shield (inside and outside) shows a rough aspect, probably due to an initial coarse texture of the metal enlarged by the dynamic strains suffered by the material.
- The ACS remained securely bolted to the roof during the test. The cylindrical wall has been deformed showing a radial bulge of 6,4 % near the top and a smaller bulge near the base ; there is no evidence of buckling. The base plate of the ACS has buckled however, and projects below the base line of the wall. The ACS total height is then greater by 2.4 % while the cylindrical wall height has reduced by 2.6 %.
- The core support has not suffered any deformation.

The most important results obtained in MARA 10 are summarized in table 1 ; corresponding results from the MARA 08 and MARA 04 tests are also included.

Concerning the global axial movement, the diagrid and vessel base displacements obtained in MARA 10 are similar to those of MARA 04.

Due to strain energy absorbed by internals, the radial shield and ACS, the roof displacement and the vessel radial deformations are smaller in MARA 10 than in the earlier bare tank MARA 08 test.

But the most important difference between MARA 10 and MARA 08 is the chronology of the roof loading : due to the presence of the ACS, the central roof is loaded from 500 µs when the first pressure peak occurs under the roof plug (see fig. 4). Hence, the roof movement begins before impact. In addition, the first impact time is delayed due to smaller fluid axial velocities. After roof impact (at about 2.3 ms), the roof, already moving, is further accelerated (see fig. 5). The roof reaches maximum displacement at about 4 ms, after which it recoils, creating a second pressure peak on the plug (see fig. 4) at about 4.7 ms ; this pressure peak slackens the downwards roof motion. After several roof oscillations, the final roof displacement is obtained at about 25. ms. We have to notice that the roof impulse on the plug is very large even though the average impulse across the roof is quite similar to the MARA 08 and MARA 04 values (see fig. 6).

4 THEORETICAL RESULTS

Precalculations of the MARA 10 test have been performed using three computer codes of different characteristics :

- SIRIUS (Lagrangian, F.D. formulation for fluid, F.E. formulation for thin shells), /5/,
- CASSIOPEE (coupled Eulerian-Lagrangian, F.D. formulation for fluid, membranes and thin shells), /6/,
- SEURBNUK/EURDYN (S/E) (Eulerian, F.D. formulation for fluid, F.E. formulation for thin shells), /7/.

The three initial calculated configurations are respectively schematized in pictures 8, 9, 10.

The SIRIUS calculation (fig. 8) needs frequent rezonings (every 100 μs) of the Lagrangian grid surrounding the bubble till the first impact occurs on the roof. This results in a 15 % loss of system energy. At 1 ms, the bubble has radially reached the shield and axially the ACS base. To continue the calculation, it is necessary to redraw the bubble boundary between the top of the shield and the lower corner of the ACS, and to assume the bubble fills the entire core region.

Rezoning problems are avoided in the CASSIOPEE calculation (fig. 9) by employing an Eulerian mesh around the inner structures.

The bubble surface has to be rezoned just before the first impact in the SEURBNUK/EURDYN calculation (fig. 10) and, more frequently, at later times.

In all codes, structures are treated with thin shells except the core support which is considered as a thick elasto-plastic material.

In CASSIOPEE and S/E, the sliding support condition between the diagrid and core support is realistically modelled, while in SIRIUS a hinge support is used instead. In all calculations, a hinge fixed condition is assumed for the roof-vessel attachment.

SIRIUS and CASSIOPEE use static material properties to describe the elasto-plastic behaviour of the various structures, while SEURBNUK/EURDYN takes into account dynamic effects assuming an average strain rate for each structure.

The main calculated results are summarized in table 2. Mesh configurations at impact time for each code are shown in pictures 11, 12, 13.

All codes predict interesting behaviour for the ACS. Early in the transient, when pressures in the core region are high, the base plate of the ACS is deflected upwards pressurising the water inside. This distorts the side wall and initiates the roof motion. After a quiescent phase, as the roof decelerates, water hammer pressures within the ACS cause further wall deformations and push the base plate back out producing buckling.

The SIRIUS calculation underestimates the axial displacements of the diagrid and vessel base because of the non realistic representation of the connection between the diagrid and core support ; otherwise, vessel hoop strains seem reasonable.

SIRIUS and CASSIOPEE underestimate the roof displacements, may be due to the uncorrect energy balance observed at the end of calculations.

Average roof impulses calculated with SIRIUS and CASSIOPEE using static material laws, are underpredicted as previously noticed in /3/.

SEURBNUK/EURDYN underpredicts the tank deformations by about 1 % absolute strain ; otherwise the results appear reasonable. The most likely causes of the discrepances are the strain rate hardening factors assumed for the dynamic material data. These data, derived from MARA 04 test measurements, /2/, correspond to average strain rates $\dot{\varepsilon} = 30$, 80 sec^{-1} respectively for the lower and upper bulge regions. However, the rates of strain are lower for MARA 10 (18, 36.sec^{-1}), and hence the hardening effect has been overestimated.

5 CONCLUSIONS

From the MARA 10 integral model experiment, we can notice that the primary containment, vessel and roof, is globally protected by the presence of internal deformable structures.

But very important effects, due to the structures surrounding the bubble, have to be pointed out :

- a delayed impact time,
- a higher total loading on the roof plug,
- a roof loading and a roof motion prior to impact.

As a consequence, the global damage of the slug impact loads on the roof are reduced taking into account core surrounding structures but local effects are more important, especially the roof plug load, /8/.

The code comparisons, obtained from three precalculations of various characteristics, show some discrepances explained by either uncorrect modelizations or non realistic assumptions on material properties. Nevertheless it seems that calculated results would be probably improved taking into account realistic strain rate effects on the material behaviour.

In addition, we have to notice that this type of problem is very severe for code calculations, especially with a Lagrangian model.

REFERENCES

/1/ D. Acker, A. Benuzzi, A. Yerkess, J. Louvet, "MARA 01/02, Experimental validation of the SEURBNUK and SIRIUS containment codes", 6th SMIRT, Paris, 1981, E3/6.

/2/ B.L. Smith, C. Fiche, J. Louvet, A. Zucchini, "A code comparison exercise based on the LMFBR containment experiment MARA 04", 8th SMIRT, Bruxelles, 1985, E4/7.

/3/ C. Fiche, J. Louvet, B.L. Smith, A. Zucchini, "Theoretical experimental study of flexible roof effects in an HCDA's simulation", 8th SMIRT, Bruxelles, 1985, E4/5.

/4/ F. David et al, "Etude d'une composition explosive flegmatisée. Applications à la déformation d'une cuve", Symposium hautes pressions dynamiques, Paris, 1978.

/5/ Y. Blanchet, P. Obry, J. Louvet, "Treatment of fluid structure interaction with the SIRIUS computer code", 6th SMIRT, Paris, 1981, B8/8.

/6/ J. Graveleau, P. Louvet, "Calculation of fluid structure interaction for reactor safety with the CASSIOPEE code, 5th SMIRT, Berlin, 1979, B1/7.

/7/ B.L. Smith, A. Yerkess, V. Washby, "The computer code SEURBNUK-EURDYN : First release version, 9th SMIRT, Lausanne, 1987, E6/6.

/8/ J. Gvildys, "Parameter studies to determine sensitivity of slug impact loads to properties of core surrounding structures", 8th SMIRT, Bruxelles, 1985, E4/6.

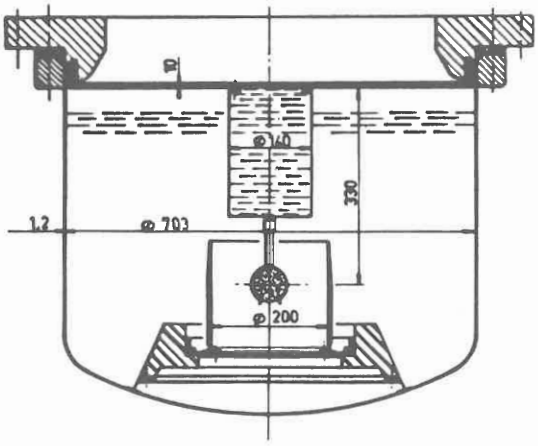

Fig:1 MARA 10

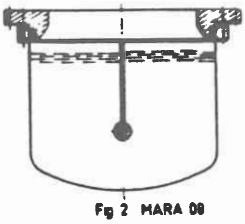

Fig 2 MARA 08

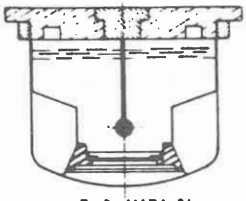

Fig 3 MARA 04

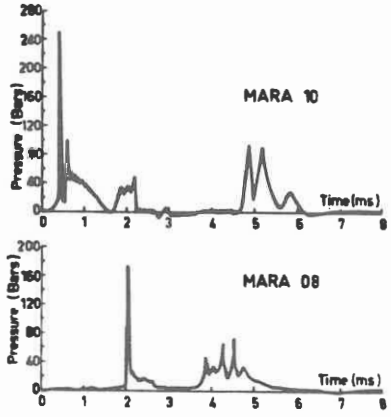

Fig:4 Selected pressure histories recorded under the roof near the axis

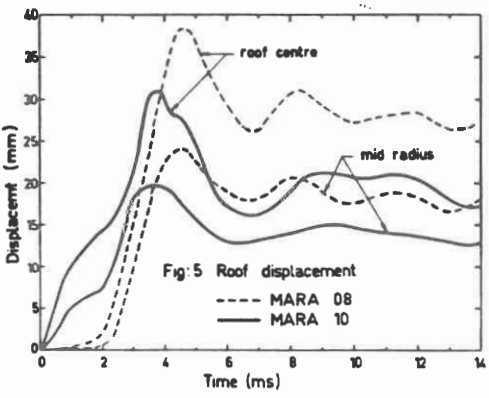

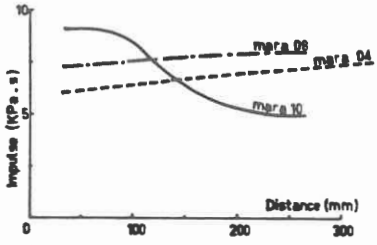

Fig:6 Recorded impulse at 8ms versus the distance from the axis

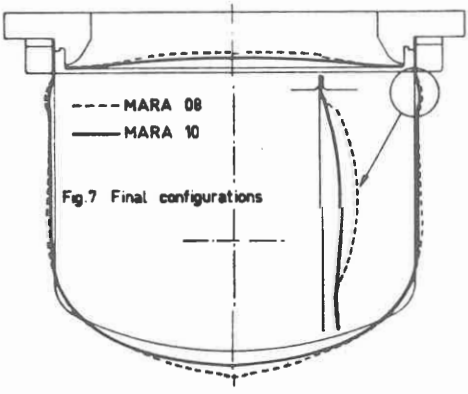

Fig:7 Final configurations

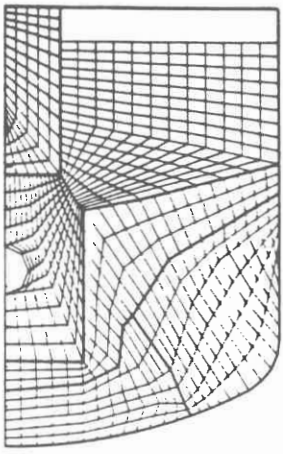

Figure 8. SIRIUS t = 0

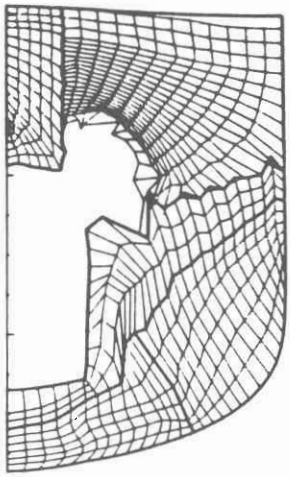

Figure 11. SIRIUS t = 2.5 ms

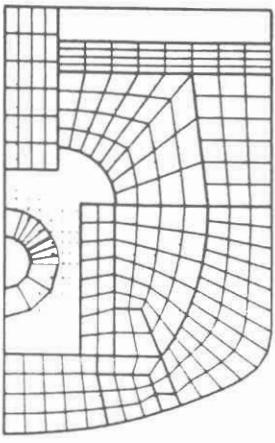

Figure 9. CASSIOPEE t = 0

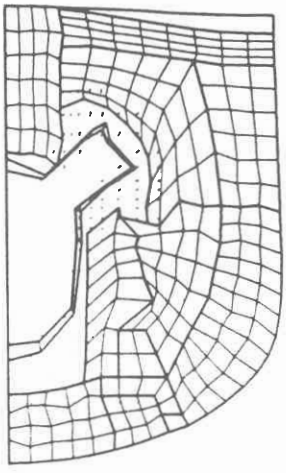

Figure 12. CASSIOPEE t = 2.5 ms

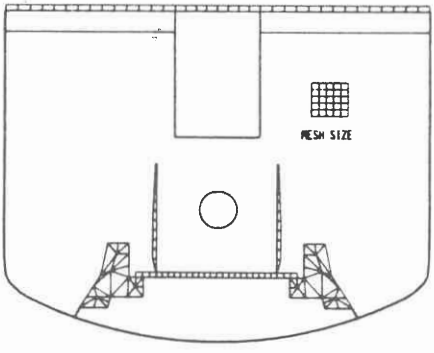

Figure 10. SEURBNUK/EURDYN
t=0

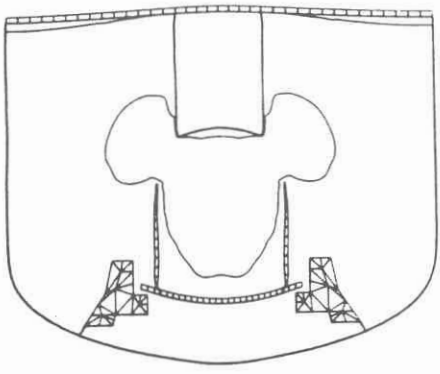

Figure 13. SEURBNUK/EURDYN
t= 2.5 ms

TABLE 1 EXPERIMENTAL RESULTS		MARA 10	MARA 08	MARA 04
Vessel hoop strain at upper bulge (%)	max	2,9	5,4	3,6
	final	2,7	4,6	3,4
distance from the roof (mm)		63,6	47,5	58,0
Vessel hoop strain at lower bulge (%)	max	1,7	5,0	3,5
	final	1,3	4,2	2,7
Vessel base displacement (mm)	max	37,9	56,0	38,6
	final	26,9	51,7	28,4
Roof center displacement (mm)	max	30,7	38,5	—
	final	18,8	27,6	—
Roof displacement at mid radius (mm)	max	19,6	24,2	—
	final	14,1	20,1	—
Diagrid central displacement (mm)	final	31,3	—	32,0
Diagrid central deflection (mm)	final	19,0	—	16,7
Hoop strain (%) radial shield	final	4,2	—	—
Hoop strain (%) inner vessel	final	—	—	12,0
Average roof impulse (KPa.s)		6,1	8	6,6
time to first roof impact (ms)		2,35	2	1,7

TABLE 2 THEORETICAL EXPERIMENTAL MARA 10 COMPARISONS		SIRIUS	CASSIOPEE	SEURBNUK EURDYN	EXPERIMENT
Vessel hoop strain at upper bulge (%)	max	2,6	3,5	1,8	2,9
	final	2,4	3,3	1,6	2,7
distance from the roof (mm)		56,0	60,0	66,0	63,6
Vessel hoop strain at lower bulge (%)	max	1,0	2,4	0,5	1,7
	final	0,8	2,2	0,4	1,3
Vessel base displacement (mm)	max	22,1	34,2	22,8	37,9
	final	17,2	28,0	17,7	26,9
Roof center displacement (mm)	max	22,5	20,3	31,7	30,7
	final	18,5	16,6	*	18,8
Roof displacement at mid radius (mm)	max	15,3	13,4	21,3	19,6
	final	12,4	10,6	*	14,1
Diagrid central displacement (mm)	max	27,5	42,5	30,6	–
	final	19,5	33,0	18,9	31,3
Diagrid central deflection (mm)	max	16,0	23,7	26,1	–
	final	14,3	22,8	23,4	19,0
Hoop strain (%) radial shield	max	6,2	6,0	5,4	6,0
	final	6,0	5,8	5,2	4,2
ACS upper bulge (%)	final	3,4	6,0	3,1	6,4
ACS wall buckling (%)	final	– 2,4	–1,3	– 1,4	– 2,6
Average roof impulse (KPa.s)		5,3	4,7	5,9	6,1
time to first roof impact (ms)		2,5	2,5	2,5	2,35

* not avalaible